7-1-2010

Assessing the Short-Term Forecast Capability of Nonstandardized Surface Observations Using the National Digital Forecast Database (NDFD)

Joby Hilliker
West Chester University, jhilliker@wcupa.edu

G Akasapu

G S. Young

Recommended Citation
Hilliker, J., Akasapu, G., & Young, G. S. (2010). Assessing the Short-Term Forecast Capability of Nonstandardized Surface Observations Using the National Digital Forecast Database (NDFD). *Journal of Applied Meteorology and Climatology, 49*(7), 1397-1411. http://dx.doi.org/10.1175/2010JAMC2137.1

JOURNAL OF GEOPHYSICAL RESEARCH, VOL. 100, NO. B9, PAGES 17,659–17,670, SEPTEMBER 10, 1995

An improved method for determining and characterizing alignments of pointlike features and its implications for the Pinacate volcanic field, Sonora, Mexico

Timothy M. Lutz

Department of Geology and Astronomy, West Chester University, West Chester, Pennsylvania

James T. Gutmann

Department of Earth and Environmental Sciences, Wesleyan University, Middletown, Connecticut

Abstract. We present an improved method for determining statistically significant alignments of pointlike features. One of the principal such methods now in use, the two-point azimuth method, depends on a homogeneous distribution of points over the region of interest. Modification of this approach by use of the relatively new statistical technique of kernel density estimation permits treatment of heterogeneous point distributions without introducing substantial dependence on choice of the grid employed in the test for significance of apparent preferred orientations. The improved method can selectively reveal alignments on different spatial scales and can suggest the locations of alignments as well as their orientation. We use this method to analyze the spatial distribution of 416 vents, largely of Pleistocene age, in the Pinacate volcanic field, Sonora, Mexico, just east of the northern end of the Gulf of California. Apart from a few sets of aligned cinder cones, the distribution of Pinacate vents appears nearly random on aerial and space photography. However, when treated statistically, old Pinacate vents exhibit structural control trending approximately N10°E throughout the field and in all its subareas. In contrast, vents with ages estimated by comparison with dated cones to be younger than about 0.4 Ma show not only the N10°E control but also N20°W and N55°W alignments significant at the 95% confidence level. The N10°E alignment probably reflects the current Basin and Range horizontal stress regime in this particular area, which is atop the mantle magma source of the Pinacate lavas. The N55°W direction is related to a major regional fracture of that orientation passing through the middle of the field and possibly related to normal faults associated with opening of the adjacent Gulf of California. The distribution of vents relative to the fracture trace is consistent with magma having been guided upward along a SW dipping fault plane. The origin of the N20°W alignment is unknown but of pre-Pleistocene heritage. We found no evidence to support control of the Pinacate vent alignments parallel to rifting or transform directions in the adjacent Gulf. Intrusion along N20°W and N55°W fractures at or since about 0.4 m.y. ago could reflect either a shift in the crustal stress field or an increase in magma pressure in Pinacate conduits that allowed magma to ascend along structures that were not parallel to the maximum horizontal compressive stress.

Introduction

The spatial distribution of volcanic vents reflects both magma source distribution and control of magma ascent by regional stresses and structures. Methods for detecting and characterizing volcanic vent alignments provide information about one aspect of volcanic vent distributions. The two-point azimuth method [*Lutz*, 1986] has been used to determine the orientations of alignments [*Wadge and Cross*, 1988, 1989; *Connor*, 1990; *Connor et al.*, 1992]. The method involves the frequency distribution of the azimuths defined by lines connecting all possible pairs of vents. As originally employed, this method did not find the locations of the alignments or the scale of the alignments, nor did it take into account other aspects of the spatial distribution, such as heterogeneities in vent density unrelated to alignments.

Other methods take into account other aspects of vent alignments. The Hough transform method [*Wadge and Cross*, 1988; *Connor*, 1990; *Connor et al.*, 1992] and the strip-filter method [*Zhang and Lutz*, 1989] have been used to determine the locations of alignments as well as alignment directions. Two-dimensional Fourier analysis has also been applied to volcanic vents [*Zhang*, 1991; *Connor*, 1990] and can yield some information about vent alignment directions and locations, although the locations of the alignments suggested can have a spuriously regular spacing because of the periodic functions involved. *Connor* [1990] integrated many of these methods and applied spatial cluster analysis as a means of separating clusters of vents that could result from time-space patterns in volcanic activity within a large field.

In some cases, the various methods of seeking alignments, applied to the same data, can provide an overall picture of alignment directions and locations. However, none of these

Paper number 95JB01058.
0148-0227/95/95JB-01058$05.00

methods explicitly takes into account the fact that alignments within a volcanic field can develop at different spatial scales. The possibility that different methods could separate alignments on different scales in some circumstances was suggested by *Zhang and Lutz* [1989]. In the present study, we develop refinements to the two-point azimuth method that can selectively reveal alignments on different scales and can suggest the locations of alignments as well as their orientation. By providing a quantitative basis for studying scales of alignments, these refinements may provide greater insight into the mechanisms by which alignments form. For example, the influence of regional structures on the distribution of vents in volcanic fields can be compared with the more local effects of dike emplacement on the formation of lines of vents.

Two-Point Azimuth Method Using Kernel Density Estimation

Lutz [1986] presented a method to estimate the statistical significance of alignments of points based on the statistics of the azimuths of line segments connecting every possible pair of points in a set. This procedure is generally known as the two-point azimuth method [*Wadge and Cross*, 1988, 1989; *Connor*, 1990]. Peaks in the frequency distribution of the azimuths are expected to result from preferred alignments of points in response to structural control [*Lutz*, 1986]. The azimuths at which peaks occur correspond to compass directions in which points tend to be preferentially aligned.

To determine whether peaks in the frequency distribution result from significant alignments of points, the observed distribution is compared to frequency distributions from Monte Carlo simulations for which points are assigned randomly to a region with the same shape as the real area of interest [*Lutz*, 1986]. If the data points are approximately homogeneously distributed, the simulated points can be generated based on a homogeneous Poisson model. *Lutz* [1986] suggested that if the data points were inhomogeneously distributed, the region could be divided into subregions in which the points were nearly homogeneous.

A more general strategy is to compare the observations to a Monte Carlo model that incorporates variations in the areal density of the points. A three-dimensional analog of this approach was used by *Fehler et al.* [1987] in applying a three-dimensional extension of the two-point azimuth (TPA) method to earthquake hypocenters. *Wadge and Cross* [1989] used this approach in two dimensions in their study of volcanic vents in the Pinacate field. In these implementations, the region is subdivided into cells on a rectangular grid, and each cell is assigned a Poisson density equal to the number of observed points divided by the area of the cell. The set of cell densities that covers the entire region is called the density model for the region. Randomly assigning points to the region based on the Poisson probabilities will statistically reproduce variations in areal density on scales larger than the cell size.

A weakness of density models defined by grid cells is that the cell densities depend on the placement of the grid relative to the points. Small shifts in the location of the grid (Figure 1) or changes in orientation can yield significantly different models. Thus, for a defined cell size the model is arbitrarily dependent on grid placement. A further weakness is that the scale on which a grid model smoothes heterogeneities is the same as the scale on which the density model is defined. As a result, the densities may vary abruptly from cell to cell. This is clearly an artifact of the modeling procedure, since the actual density of points might be a smoothly varying function of position and any actual discontinuities would only coincidentally be related to the cell edges.

The kernel density estimator used in this paper yields areal density models that are not strongly affected by the deficiencies of the grid cell method. *Silverman* [1986] reviews the literature on the relatively new field of kernel density estimation.

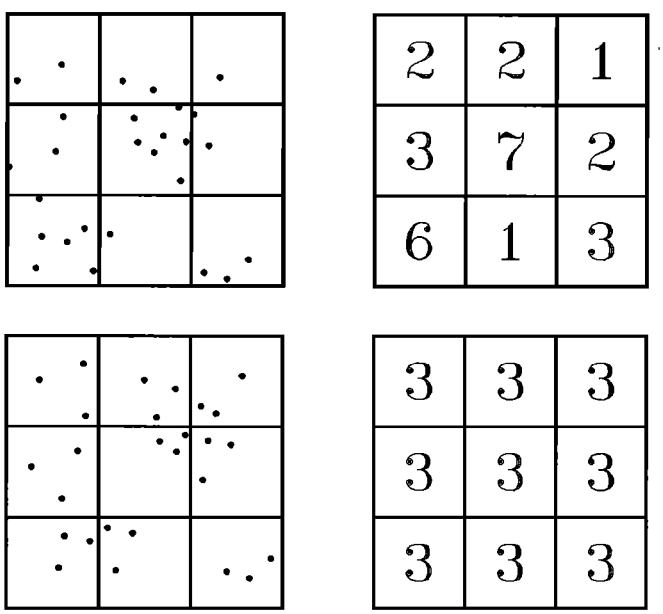

Figure 1. Effect of grid placement on grid cell density estimates. (top right) Areal density (points/unit area) for a grid placed on a set of points (top left). (bottom right) Areal density that results if the grid is translated down and to the left by ¼ of the grid spacing in each direction (bottom left).

The concept of a kernel estimator can easily be visualized in one dimension (Figure 2). Imagine that a symmetrical function, called the kernel function, is placed at the coordinate of each datum. The sum of the kernel functions over all the data is an estimate of the density. In mathematical terms, the resulting density model can be thought of as the convolution of the data with the kernel function.

The half width h of the kernel function determines the degree to which individual data are resolved (Figure 2). A range of widths provides a set of models (e.g., Figures 2a-2d). In this example, data, or groups of data, which are separated by more than $2h$ are perfectly resolved by the model (e.g., all data in Figure 2a; groups 1+2, 3+4+5, and 6 in Figure 2c). Data separated by less than about $1.4h$ are not resolved (e.g., no data or groups in Figure 2d). Thus increasing h yields smoother models that only resolve the larger-scale features of the data.

When applied to points in a plane, the kernel function smoothes the data in two dimensions. We use the two-dimensional analog of the quadratic kernel shown in Figure 2, the bivariate Epanechnikov kernel [*Silverman*, 1986]. This kernel function has a high statistical efficiency and involves a relatively low degree of computational effort. The density model consists of the density values in every cell of a rectangular grid that spans the sample region. The linear density in any particular cell is the sum of the kernel functions of all the data, evaluated at that cell's center.

The advantages of the kernel estimator derive from the fact that the scale on which the model is gridded can be independent of the width of the kernel used to smooth the data. In particular, the grid cells can be made much smaller than the half width of the kernel function. If the grid spacing is less than h, the maximum half width of the kernel, the density model is insensitive to the orientation and location of the grid. The grid spacing can be made as small as practicable, given computer resources and speed.

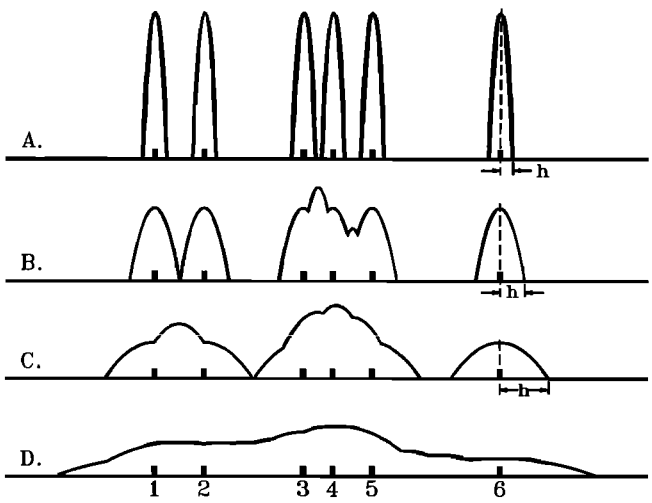

Figure 2. Kernel density estimation for univariate data using quadratic Epanechnikov functions; kernel half width h is indicated in Figures 2a, 2b, and 2c. The data are indicated by heavy vertical bars. Curves indicate the density obtained by summing the kernel functions of the six data. In Figure 2a, the kernel half width h is 40% of the distance between the closest points. In each of the succeeding models (Figures 2b, 2c, and 2d) the kernel width is increased by a factor of 2.

Although methods exist to choose an optimal kernel width with regard to particular measures of statistical performance, they do not interest us here. Rather, it is the fact that kernel models with different values of h can capture different features of the data (e.g., Figure 2) that makes them extremely valuable tools to obtain density models for the TPA method. To illustrate this point, we construct a set of 65 points within a circular region (Figure 3) so that there are (1) narrow, discontinuous alignments of points in a N-S direction separated by about 1 km, on average; (2) wider NW trending bands of points that are separated by about 5-10 km; and (3) a broad (30-40 km) band of points trending NE.

By selecting different values of h, the density models (Figure 4) resolve features of the data at different spatial scales. For a density model using h=1 km (Figure 4), most points in Figure 3 are resolved individually or in pairs, and even the smallest-scale alignments are visible as N-S "strings" of high-density peaks, or elongated "hills" of high density. If h is increased to 5 km, the N-S alignments are not resolved as well (Figure 4).

For each density model in Figure 4, the corresponding two-point azimuth (TPA) analysis is presented in Figure 5. The TPA method looks for differences between data and Monte Carlo simulations based on a density model of the data. If the density model, and therefore the simulations, reproduces the data almost exactly, no differences will be found. This can be seen in the results of the TPA analysis for h=1 km in Figure 5, in which the N-S alignment of the points is not significant relative to the simulated points. The TPA analysis detects dif-

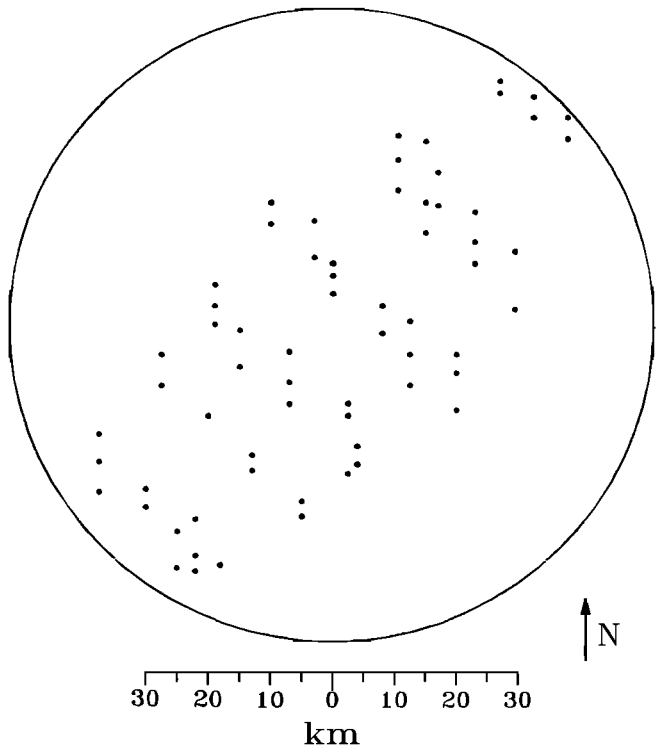

Figure 3. Locations of 65 points used to demonstrate the influence of kernel half width h on density models (Figure 4) and TPA analyses (Figure 5). Points are arranged in short (two to three points) N-S alignments and NW trending bands and form an overall NE trending group. The density models and simulations for the TPA method are carried out within the region enclosed by the circle.

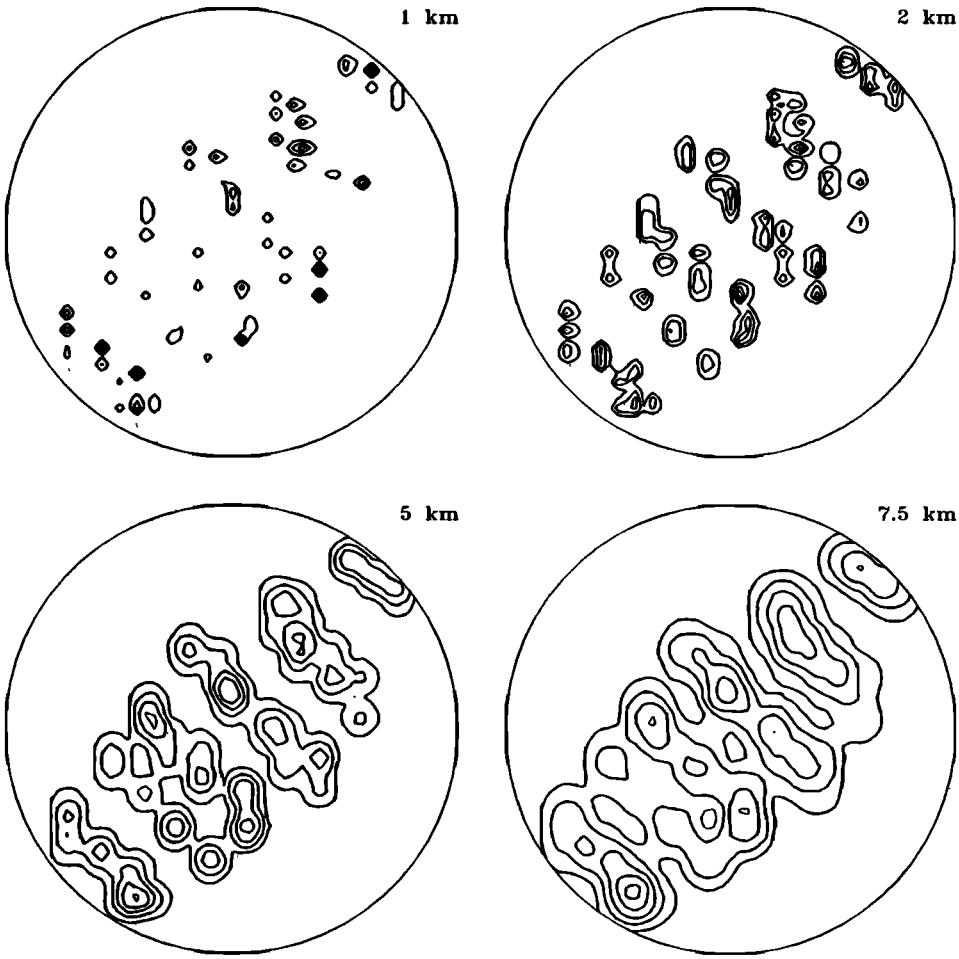

Figure 4. Contour line representations of kernel density models for the points in Figure 3. Values of h are indicated next to each model. The contours are estimates of point density corresponding to 10%, 30%, 50%, 70%, and 90% of the maximum density.

ferences between the data and the simulations if the alignments in the data are more closely spaced than the kernel half width used in the density model. When h is 2 km, the N-S alignments in the data (separated by about 1 km) become significant relative to the simulations (Figure 5). Confidence levels are estimated empirically from the Monte Carlo simulations [*Lutz*, 1986].

The density model for h=5 km (Figure 4) clearly reveals the wider, NW bands. Consequently, when this model is used to simulate points for the TPA analysis, significant NW alignments are not found; only the smaller-scale N-S alignments appear (Figure 5). For h=10 km and h=15 km the NW bands are not separated well (Figure 4). TPA analyses using these models show that a NW peak is significant at the 95% confidence level (Figure 5).

Models with h=20 km and h=30 km (Figure 4) show that these kernels are wide enough to broaden the overall NE elongation of the points. As a result, the TPA analysis reveals a significant NE alignment for models with these values of h (Figure 5). Alignments of points along this band are qualitatively different from the N-S and NW alignments because there is no intrinsic NE pattern except the elongation of the outcrop region. As a result, the NE peak on the TPA frequency distribution is broad, in contrast to the sharper N-S and NW peaks.

For the purposes of this example, we use the region enclosed by the circle in Figure 3 for Monte Carlo simulations so that the alignment effect induced by the NE band of points can be compared with the other alignments. If a region is used that fits the data more closely, the NE TPA peak can be eliminated by reducing the shape effect, as demonstrated by *Lutz* [1986].

If multiple alignments are present in a group of points, a very strong alignment with one characteristic width may diminish the apparent significance of narrower, smaller-scale alignments. For example, the N-S and NW alignments are not significant when the largest kernels are used (Figure 5). This occurs because individual large-scale alignments typically contain many more points than smaller-scale alignments and the heights of peaks in the frequency distribution are roughly proportional to the square of the number of points [Lutz, 1986]. Thus, at large kernel sizes, when alignments on all scales can compete, the wider bands with the most points dominate the frequency distribution.

This synthetic example (Figures 3-5) demonstrates how the spacing of alignments revealed by the two-point method is related to the width of the kernel. If the kernel is narrow enough to resolve alignments well, so that they are evident in the density model, the two-point azimuth method will not detect them. On the other hand, a model in which h is large

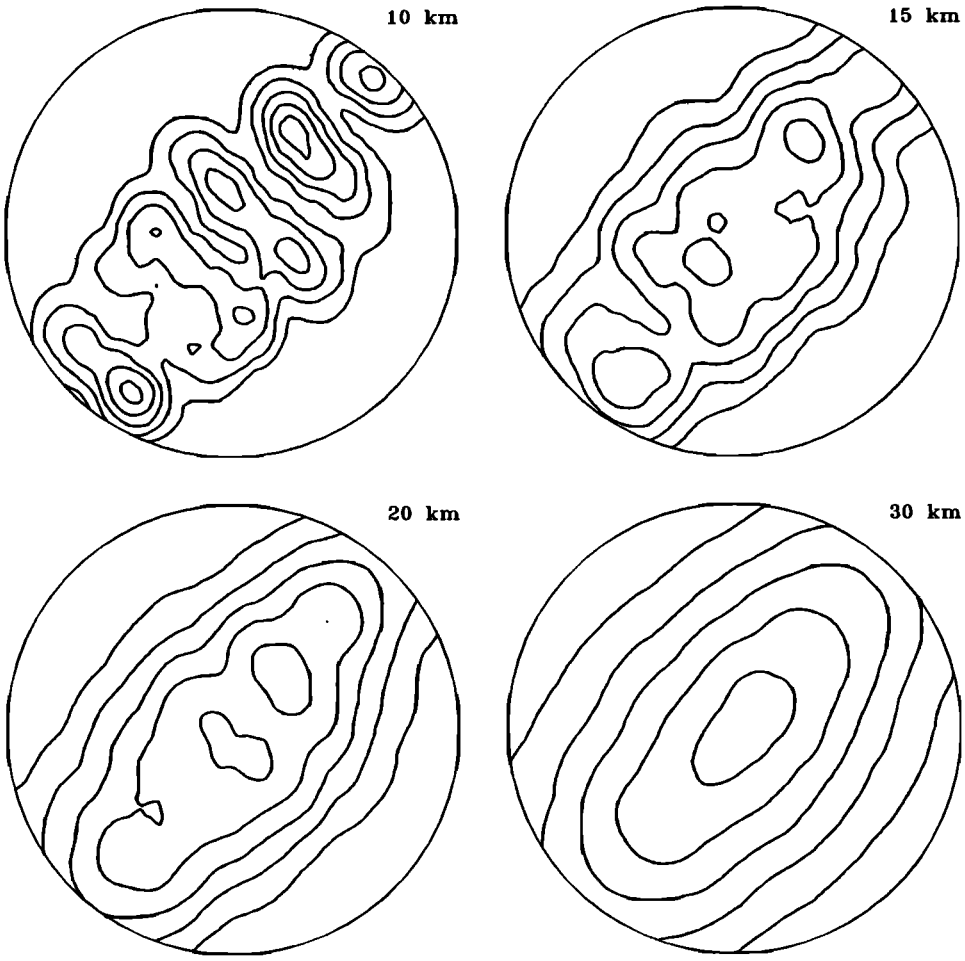

Figure 4. (continued)

enough so that the alignments are "blurred" will generally permit them to be detected by the two-point method. As a general rule, TPA analysis based on a density model with $h = h^*$ detects alignments that will appear most clearly in density models with $h < h^*$, where h^* is some particular value of h. Thus the physical locations of the data forming significant alignments are revealed by density models constructed with somewhat smaller values of h. The minimum value of h at which peaks in the TPA frequency distribution become statistically significant is comparable to the characteristic band width or spacing between bands.

A comparison of results obtained using the original TPA method to TPA analysis using kernel density estimation shows that the revised method is not merely an incremental improvement. The frequency distribution in Figure 5 for $h=\infty$ corresponds to the original TPA analysis. Note that the original method does not detect either of the two smaller-scale alignments, whereas the revised method provides information about the locations and scales of all three alignments.

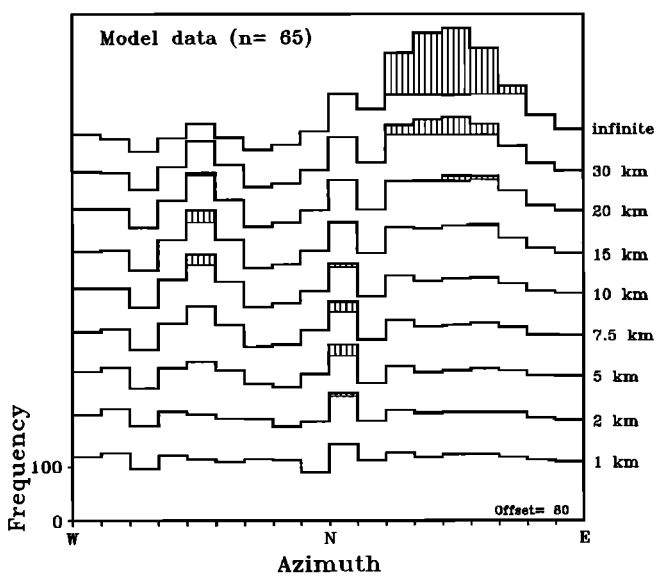

Figure 5. TPA frequency histograms for the points in Figure 3 normalized to the frequencies that result from simulations based on the density models in Figure 4. The frequency scale shows numbers of alignments with azimuths that fall within 10° histogram cells. Hatched portions of histogram cells exceed the 95% significance level.

Pinacate Volcanic Field

The Pinacate volcanic field lies in northwestern Sonora, Mexico, in the Basin and Range Province and just east of the northern end of the Gulf of California. The Pinacate is underlain by Precambrian crust, up to 1.7-1.8 Ga, and lies very near a line that marks the western limit of that crust, a line that

coincides with the apparent southward extension of the San Andreas fault system [*Anderson and Silver*, 1981]. The trace of the Mojave-Sonora megashear crops out east of the Pinacate, where it trends northwesterly and is believed to pass north of the volcanic field (T. Anderson, personal communication, June 1993).

The volcanic field comprises some 1500 km^2 of alkali basaltic rocks, including hundreds of cinder cones and nine maar craters (Figure 6). The structure and eruptive cycle of the cinder cones and the geology of the largest maar were described by *Gutmann* [1976, 1979]. *Lynch* [1981] determined K-Ar ages from the field and showed that the area contains two sets

Figure 6. Skylab 3 photograph of the Pinacate volcanic field. Heavy fiducial marks along the east and west sides are approximately along the trace of the inferred N55°W fracture zone.

of lavas: the older Santa Clara basalt-to-trachyte series, ranging in age from more than 1.7 Ma to 1.1 Ma, and the younger Pinacate series, of which the oldest dated unit is 1.2 Ma. The youngest Pinacate series vents appear to be no more than a few thousand years old.

In the southern part of the volcanic field, the Santa Clara series forms a trachyte shield massif that is deeply eroded in many places and mantled by the younger lavas of the Pinacate series [*Lynch*, 1981]. The southern half of the field is dominated topographically by the Sierra Pinacate, which rises to 1206 m (at Pinacate Peak) above the Gulf of California about 35 km to the southwest. The numerous cinder cones and maars of the Pinacate field, including most, if not all, of the vents referred to in this report, belong to the Pinacate series.

Further details and a general description of the volcanic field are provided by *Lynch and Gutmann* [1987]. Alignments of Pinacate cinder cones were studied previously by *Wadge and Cross* [1989], who reported the presence of N-S directional control.

Procedure for Locating and Characterizing Vents

The vents were located on aerial photographs (approximate scale 1:62,500) and plotted on Mexican SPP (Secretaria de Programacion y Presupuesto) topographic maps (1:50,000; 20-m contour interval). Vents were omitted if they could not be located within about 100 m or if they occur off the 1:50,000 topographic base maps, are outliers on the borders of the field far from other vents, or are very small and possibly pseudocraters. Multiple vents from a single eruptive center were mapped individually where well defined. The locations of 416 vents were determined.

The vents were classified into one of three age categories (young, intermediate/ indeterminate, and old) based on the degree of erosional modification and on stratigraphic relationships observed on stereo pairs and in the field. Several factors make age estimation difficult and uncertain. Variation in the aspect ratios of Pinacate cones probably resulted locally from syneruptive processes and not just from erosion. Some Pinacate cinder cones contain a higher proportion of erosion-resistant, agglutinitic ejecta than others. Differences in cinder cone structure, in emplacement of dikes and sills, and in the degree of dismemberment by breaching flows [*Gutmann*, 1979] add further variability and uncertainty. Our classification doubtless involves some errors in such a large population of cones, but this problem could only be solved by very numerous absolute age determinations. Our "young" versus "old" characterizations should be valid for most vents.

Young cones are those which show well-defined cone shape and relatively modest dissection by erosion. The slopes of these cones can have deep rills but generally lack the sharply curving, large gullies that develop on the old cones. The outward dipping parts of their agglutinitic ruffs [*Gutmann*, 1979] may be removed by erosion, but the cone rims commonly remain well defined. Based chiefly on these criteria, 120 vents are tentatively identified as young. The shapes of cones in the old category have been substantially modified by erosion and are cut by deep, curving gullies; and their associated flows are thickly mantled with younger material (erosional or airborne debris or lava flows). About half the vents (204) are classified as old. Age assignments qualified with a question mark carry a relatively high uncertainty.

The 92 vents that are classified as of intermediate/indeterminate age either have characteristics that are intermediate between cones of the old and young categories or are so small or so concealed by younger units that their relative age cannot be estimated. Many of the vents in this category probably are of intermediate age but some vents that are quite old or quite young might be included as well.

Electronic supplement Table 1[1] gives the locations of the 416 vents together with K-Ar ages from *Lynch* [1981] and *Slate et al.* [1991]. The ages of three dated cinder cones in the young category range from 0.14 to 0.34 Ma, and the ages of two cones in the old category are 0.46 and 0.48 Ma. The source vents for several Pinacate flows ranging in age back to 1.2 Ma [*Lynch*, 1981] could not be located. Two cones with intermediate characteristics have K-Ar ages in the range of 0.41-0.46 Ma consistent with an intermediate age. It seems likely that the ages of vents in the young category are generally less than about 0.4 Ma, while the ages of those in the old category are chiefly more than about 0.4 Ma.

Results

We analyze the young and old vents separately to assess whether or not controls on vent location were the same for both age groups. Changes in the orientation of the horizontal principal stresses could have occurred on the 10^4-10^5 year timescale as a result of tectonic processes operating along the Gulf of California-San Andreas plate boundary. Furthermore, the magma pressure in Pinacate conduits might have changed relative to the magnitude of the horizontal stresses. For example, an increase in magma pressure could allow magmas to ascend along fractures with new orientations [*Delaney et al.*, 1986].

A map of the vents (Figure 7) shows that the Pinacate field is not uniformly populated with vents. A notable feature of the vent distribution is a northwest trending band, densely populated with vents, that runs through the center of the field. Immediately south of this band, and parallel to it, is a region with relatively few vents. These features suggest that the parts of the Pinacate field to the north and south of the region with few vents might be different from one another. For example, the north and south regions might be underlain by basement rocks that experienced different tectonic histories. We test this possibility by analyzing vents in the north and south regions separately.

We use a similar set of parameters in each analysis to make the results easier to compare. The density models are computed with a grid spacing of 0.75 km, small enough to ensure insensitivity to the location and orientation of the grid for the range of kernel widths (h= 5-15 km) used. Each vent was assigned a radial location uncertainty. Our conclusions are insensitive to the exact value of the uncertainty on a range from 0 to 500 m; an uncertainty of 50 m is used for the results pre-

[1]An electronic supplement of this material may be obtained on a diskette or Anonymous FTP from KOSMOS.AGU.ORG. (LOGIN to AGU's FTP account using ANONYMOUS as the username and GUEST as the password. Go to the right directory by typing CD APEND. Type LS to see what files are available. Type GET and the name of the file to get it. Finally, type EXIT to leave the system.) (Paper 95JB01058, An improved method for determining and characterizing alignments of pointlike features and its implications for the Pinacate volcanic field, Sonora, Mexico, by T.M. Lutz and J.T. Gutmann). Diskette may be ordered from American Geophysical Union, 2000 Florida Avenue, N.W., Wasington, D.C. 20009; $15.00. Payment must accompany order.

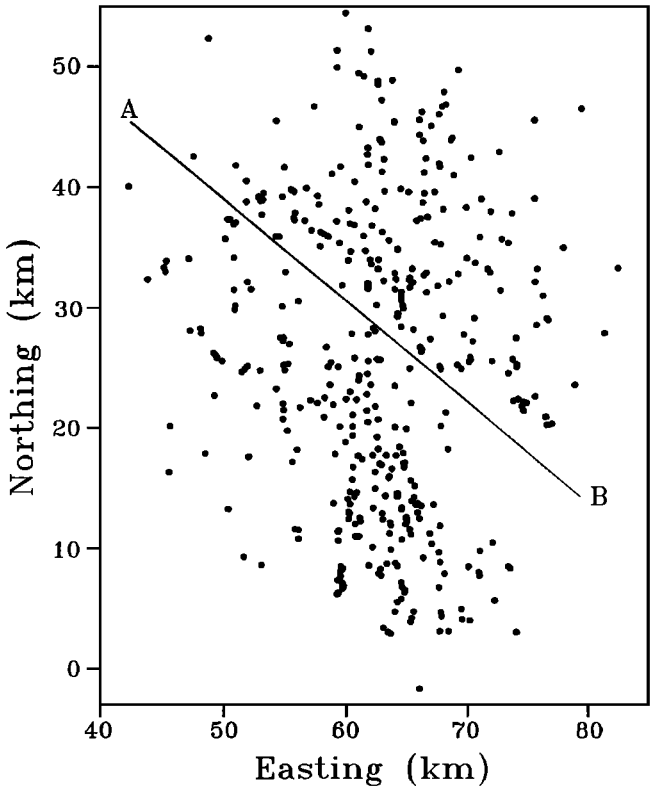

Figure 7. Map of 416 Pinacate vent locations used in this study; UTM coordinates of vents are given in electronic supplement Table 1. Line A-B indicates the boundary between the north and south regions.

sented here. The azimuthal frequency distributions are tabulated in 10° bins. Directions of vent alignment referred to in this study are considered to have uncertainties of ±10° (i.e., N10°E indicates alignments oriented N-S to N20°E).

Results for all of the old vents demonstrate a N10°E orientation of vent alignments (Figure 8a). Results for old vents in the south region (Figure 8b) and the north region (Figure 8c) both confirm the presence of significant alignments oriented approximately N10°E. In the south region, alignments are only detected with $h \geq 5$ km, and the peak remains narrow for h up to 15 km, suggesting that the alignments are separated by less than 5 km. In the north region, the alignments are only detected for $h \geq 7.5$ km, and the width of the peak increases rapidly with increasing h. These results show that the alignments in both regions have the same orientation and suggest that the stress conditions and orientations of crustal fractures were the same in both regions. The differences between the results might be related to differences in the type of fractures that formed. For example, the thick Santa Clara volcanic pile that underlies the southern part of the field might have fractured differently from the crust to the north.

Results for the young vents reveal a different and more complicated picture. Alignments are detected with several different orientations, roughly N10°E, N20°W, and N55°W. When all young vents are considered, significant N10°E and N20°W alignments are revealed (Figure 9a). A N55°W peak is present consistently for all values of h but does not exceed the 95% confidence level.

Analysis of the young vents in the north and south regions separately reveals that the N55°W alignment is associated with the NW trending band of vents that crosses the field (Figure 7). The vents in the north region, which include this band, show a significant N55°W alignment (Figure 9c) but young vents in the south region do not (Figure 9b). However, if the 34 young vents in the band are included in the south region, the N55°W alignment appears (Figure 10).

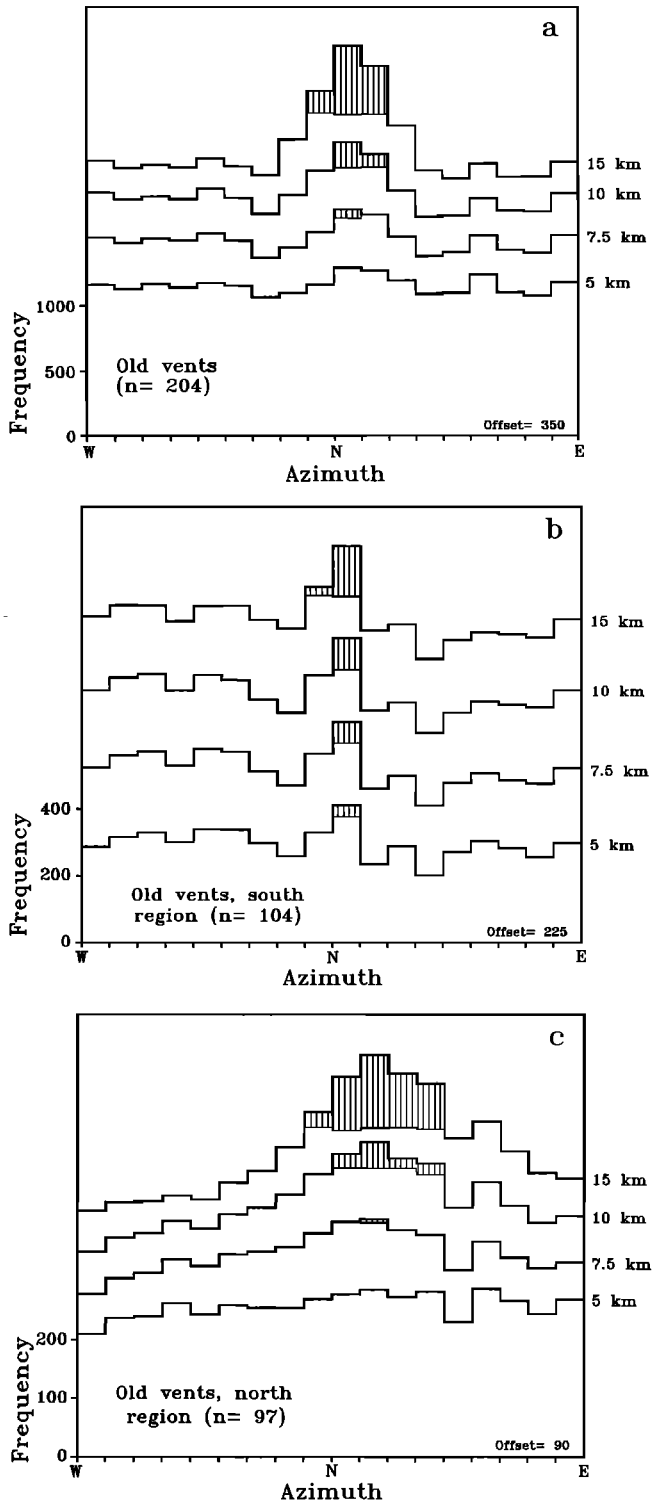

Figure 8. TPA frequency histograms for old vents: a. All old vents. b. South region. c. North region. A total of three outlying points are excluded from Figures 8b and 8c. The frequency scale shows numbers of alignments with azimuths that fall within 10° histogram cells. Hatched portions of histogram cells exceed the 95% significance level.

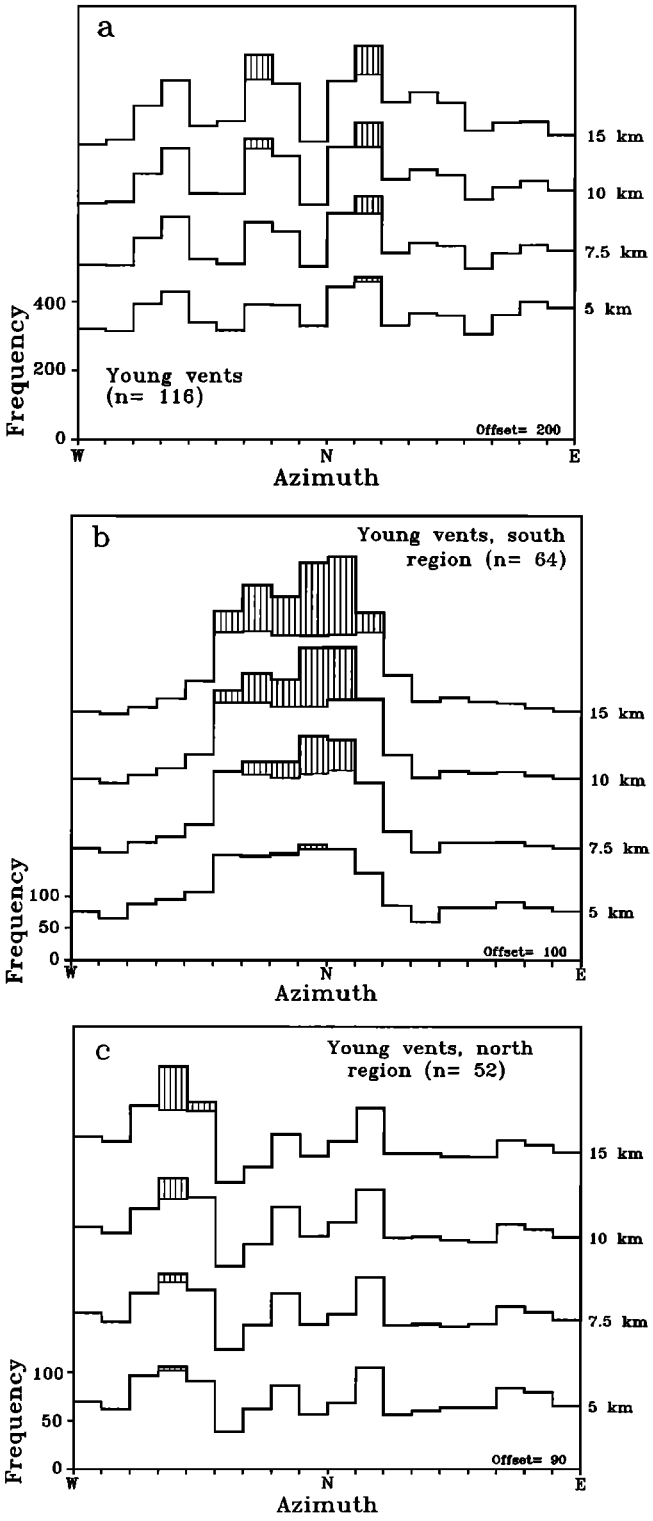

Figure 9. TPA frequency histograms for young vents: a. All young vents. b. South region. c. North region. Four outlying vents are excluded. The frequency scale shows numbers of alignments with azimuths that fall within 10° histogram cells. Hatched portions of histogram cells exceed the 95% significance level.

Discussion

The relative motion between the Pacific and North American plates in this area is expressed by the axis of spreading in the Gulf (N52°E) and transform motion (N38°W). The prevailing trend of the Basin and Range mountain blocks in the vicinity is approximately N35°W. None of these directions appears as a statistically significant frequency peak in any of the TPA plots of Pinacate vents. It appears that current plate margin tectonism did not directly control the alignments of the Pinacate vents.

The presence of short, N-S lines of penecontemporaneous vents in the Pinacate was noted by *Lynch* [1981]. *Wadge and Cross* [1989] studied the spatial distribution of Pinacate vents located on satellite images using the TPA method [*Lutz*, 1986] and the Hough transform method. They concluded that only N-S alignments of vents are present. There are two main reasons why the results of the present study differ from those of Wadge and Cross. First, their data consisted of vent locations without relative ages. Alignments trending N20°W and N55° W are found only in the young vents. When all vents are analyzed together without regard to age, only the N-S alignments are detectable (Figure 11). Second, Wadge and Cross modified the TPA method by introducing a rectangular grid with an 11-km spacing to obtain a density model. As shown earlier in this paper (Figure 1), grid models of this type are highly dependent on location and orientation. Although they do not specify the orientation of their grid, the presence of N-S grid lines could have accentuated the evidence for N-S alignments and made it more difficult to detect alignments in other orientations.

Origin of Vent Alignments

The presence of significant alignments suggests that the location of volcanic vents was controlled. In the large majority of TPA analyses performed as part of this study, significant alignments are detected only for $h \geq 5$ km. This fact suggests that the alignments do not generally consist of "perfect lines" of vents but that instead the vents form bands. The values of h at which significant alignments occur suggest that the bands are either many hundreds to a few thousand meters wide or that individual bands are separated by that much. We conclude that alignments in the Pinacate field are associated with broad linear zones in the basement rocks, or mantle, that controlled the production of magma or guided its ascent and not with laterally extensive dikes. This conclusion is consistent with the observation that linear arrays of vents are not prominent in the field or in air photos.

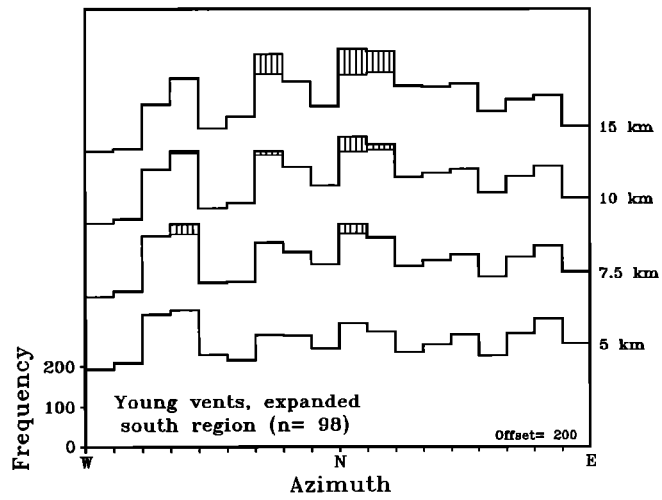

Figure 10. TPA frequency histogram for young vents in the south region plus 34 young vents that form the NW trending band.

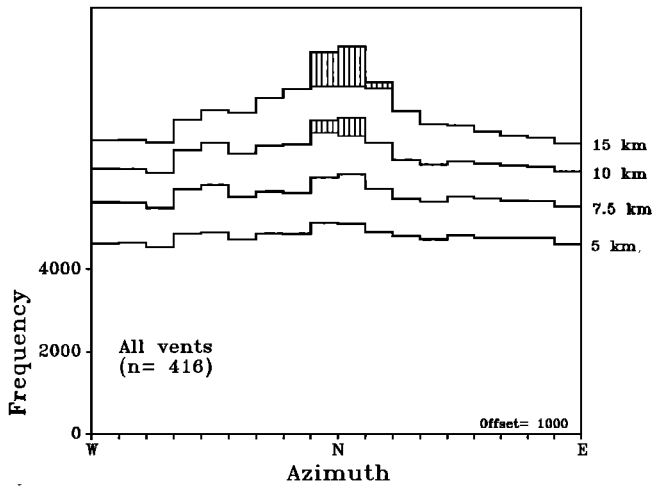

Figure 11. TPA frequency histograms for all vents in the Pinacate volcanic field.

A map of the areal density of vents with h = 3 km reveals the variations in density that accompany the significant alignments (Figure 12a). The relative areal density of Pinacate vents is contoured from 1.0 vents/unit area (where density is highest) to 0.1 vents/unit area. The contours clearly display the band of vents that largely makes up the N55°W alignment. In addition, "ridges" and strings of "hills" can be seen that follow the N20°W and N10°E trends. These observations suggest that the structural control resulted in bands of vents that are a few kilometers across, possibly reflecting fairly wide fracture zones or other linear features.

The features of vent distribution shown in Figure 12a are also reflected in the Hough transform results of *Wadge and Cross* [1989, Figure 7]. However, it is not possible to make a rigorous comparison between their results and ours because the Hough transform results depend on values selected for each of five parameters, and Wadge and Cross show results for only one set of these.

Lynch [1981] and *Wadge and Cross* [1989] suggest that the N-S alignments may reflect tension associated with shear along the San Andreas transform fault system west of the volcanic field. We suggest it is also possible that this extension may reflect tectonic processes associated with the Basin and Range mantle source region of these lavas. The Pinacate volcanic field is elongated N-S, and *Lynch* [1981] noted that 75% of Pinacate eruptive centers lie in a broad, N-S trending belt. Figure 12b shows the relative areal density of Pinacate vents computed for h=7.5 km, a width at which discrete fault zones are largely smoothed out of the density distribution. N-S elongation of the magma source is suggested by this vent density plot. In this view, the Pinacate volcanic field may reflect a local "boil" in the mantle, somewhat akin to a hot spot but more localized in space and time, that is more related to Basin and Range extension than to the spreading and transform activity a short distance to the west.

The N20°W alignment corresponds with the trend of the long axis of the Santa Clara trachyte shield. The elongation of that massif indicates that N20°W control was important when the shield was formed, more than 1.1 Ma [*Lynch*, 1981]. The origin of this control is unknown at present. Judging from the TPA plots, N20°W directional control of the young vents appears stronger in the south region than in the north region. However, none of the TPA results or the density maps support the idea that the southern and northern parts of the Pinacate are underlain by structurally dissimilar basement terrains.

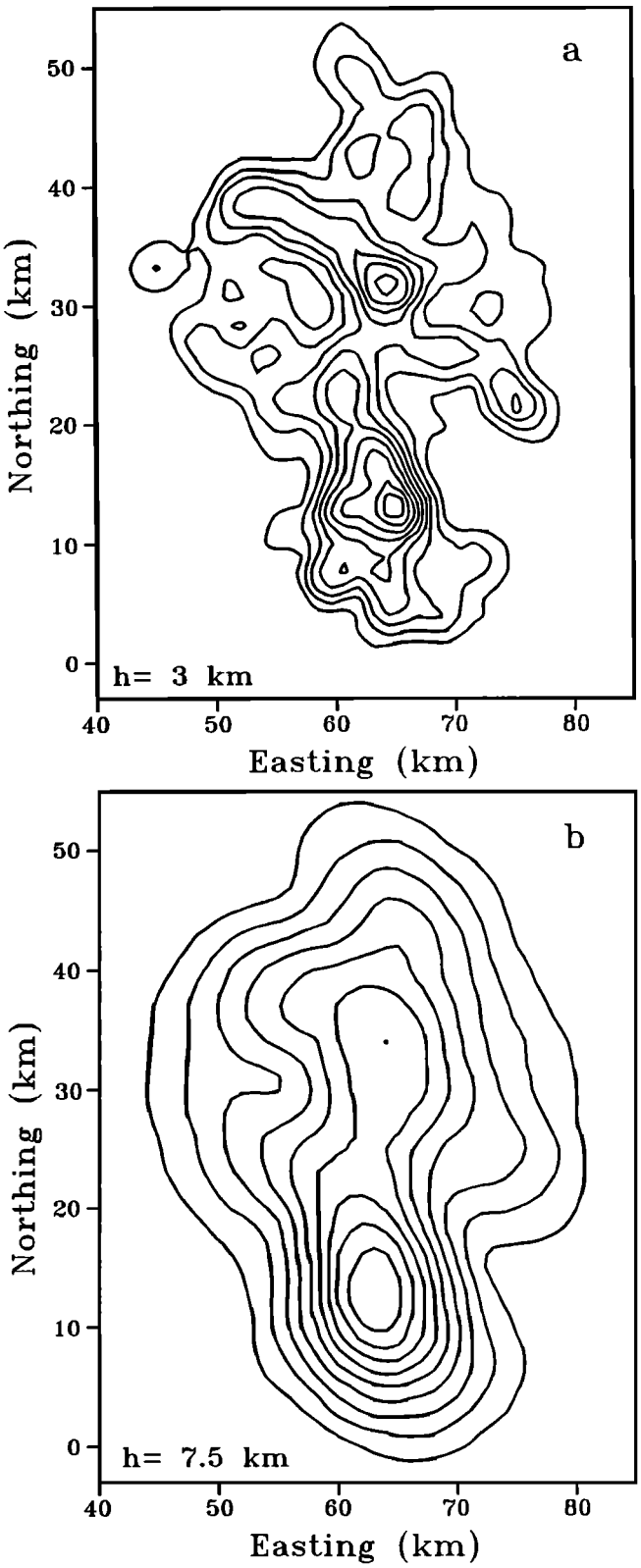

Figure 12. Maps of relative areal density of vents in the Pinacate field; contours are at intervals of 10% of the maximum density, from 10% through 90%. (a) h = 3 km; (b) h = 7.5 km.

The strong N55°W directional control shown by relatively young vents in the north region probably reflects in large part a belt of 34 vents that extends across the field from the vicinity of Crater Elegante to and beyond MacDougal Crater. Exposed in the walls of Sykes Crater, one of the young maars in this belt, is a steeply dipping and laterally extensive dike trending about N56°W. The minimum values of h at which a significant N55°W peak appears suggest that the alignment is due to a belt or belts about 5 km wide. Adjacent to and SW of this belt is a parallel zone that is largely devoid of vents.

If the N55°W trending belt is extended northwestward about 20 km along strike, it intersects the southeastern end of the Tinajas Altas Mountains. R. Merriam (personal communication, August 1992) mapped a fault there that cuts pre-Cretaceous gneiss and granite and Cretaceous batholithic rocks and trends N50°-55°W. *Donnelly* [1974] also shows a fault in the southeastern Tinajas Altas Mountains and indicates that it is down to the southwest. *Fenby and Gastil* [1991] show a major regional fault here trending N55°W.

This fault is interpreted by *Gastil and Fenby* [1991] as a southwest dipping, listric normal fault believed to be related to a pre-5 Ma detachment associated with opening and tectonic filling of the Gulf of California. The N55°W fracture zone cutting the Pinacate field evidently may be an extension of this detachment fault. Its southwest dip likely accounts for the zone of few vents that is parallel to and southwest of the belt of abundant vents: Pinacate magmas would have been guided northeastward along the SW dipping fault as they ascended. Structural control of ascending magmas has been examined theoretically by *McDuffie et al.* [1994], who conclude that structures could redirect dikes as much as 3-5 km laterally. The width of the belt devoid of cones is within this range. Exploitation of faults by magmas as pathways to the surface has also been suggested by *Draper et al.* [1994] for the San Francisco Volcanic Field.

The time at which Pinacate vents began to exhibit significant N55°W and N20°W control is poorly constrained. Owing to the uncertainty of individual cone age assignments and the large number of cones involved, it seems unlikely that the timing of the change can be closely defined, even with many more absolute age calibration points. Presently available data indicate that the N-S directional control was joined by N55°W and N20°W influences about 0.3-0.5 m.y. ago.

Delaney et al. [1986] explored the relationship between horizontal principal stresses and magma pressure as it influences the orientations of fractures utilized by ascending magmas. They concluded that if the difference between the horizontal principal stresses is small relative to magma pressure, vertical dikes can intrude not only along planes perpendicular to the least compressive stress but also along fractures at lesser angles to that stress. Judging from the several short N-S lines of contemporaneous vents [*Lynch*, 1981], least compressive stress in this area evidently is oriented close to E-W. Thus magma ascent along N20°W and N55°W fractures could reflect either an increase in Pinacate magma pressure, a decrease in the horizontal principal stress difference, or both. Of the 15 K-Ar ages reported for Pinacate series lavas by *Lynch* [1981] and *Slate et al.* [1991], it is interesting to note that seven are in the range 0.41-0.48 Ma. Although this concentration could be an artifact of sampling, it is consistent with the occurrence of especially vigorous Pinacate magmatism, and possible high magma pressure, at about 0.4-0.5 Ma.

Implications for Other Methods

Connor [1990] and *Connor et al.* [1992] have applied cluster analysis to separate volcanic fields into spatial clusters, each of which can be analyzed using TPA, Hough transform, or other methods. A key aspect of this method is that it lets researchers explore the possibility that different clusters of vents could have different alignment directions. *Connor* [1990] and *Connor et al.* [1992] analyze clusters that remain stable to perturbations across a limited range of search radius, and thus study clusters of essentially a single size scale in a given field. Cluster analysis also tends to produce clusters that are roughly equidimensional, as shown by *Connor et al.* [1992, Figure 5]. The improved TPA method explicitly considers heterogeneities in vent density across a range of scales, and kernel density maps (e.g., Figure 12) suggest clusters of many sizes and shapes. However, kernel density analysis does not provide an unambiguous method to separate one cluster from another. Thus cluster analysis and kernel density maps have some complementary aspects.

The Hough transform method [e.g., *Wadge and Cross*, 1989; *Connor*, 1990] has been used to determine the locations of the vents that form alignments. The Hough transform requires that values be selected for five parameters, several of which must be chosen subjectively or are determined by experience [*Wadge and Cross*, 1989; *Connor*, 1990]. Furthermore, Hough transform analysis is sensitive to the number of vents used in the analysis and to the shape of the vent cluster. Kernel density maps provide similar information and involve fewer "educated guesses" about parameter values.

Two-dimensional spectral analysis has been used to identify alignment directions and locations [e.g., *Connor*, 1990]. Phase maps [e.g., *Connor*, 1990, Figures 6-8] provide information similar to the kernel density maps. However, phase maps are constructed directly from the high amplitude, periodic, Fourier functions and thus might contain fluctuations in density that are anomalously regular.

The analysis of the Pinacate vents makes clear the correlated but different functions of density modeling and TPA. Vent density models at any value of h usually reveal many possibly significant spatial variations in density. Which of these, if any, are significant cannot be determined by inspection of the density map alone. TPA provides a means to evaluate the significance of alignments that appear on the density maps.

Conclusions

This study develops and demonstrates a refinement of the two-point azimuth (TPA) method that has several advantages.

The new method can more accurately determine alignments of pointlike features that are heterogeneously distributed. Kernel density modeling of the data removes ambiguities that can be introduced by other approaches.

Alignments on different spatial scales can be detected and characterized.

The locations of the vents in broad alignments are indicated by kernel density maps.

Vent locations in the Pinacate volcanic field reflect a change in stress conditions at about 0.3-0.5 Ma. During this time there was an increase in the ratio of magma pressure to the difference between the principal horizontal stresses. As a result, new structures in orientations not perpendicular to the minimum horizontal compressive stress were exploited.

Among these was a N55°W trending fracture zone that may be a SW dipping listric fault associated with opening of the Gulf of California [*Gastil and Fenby*, 1991]. Structural control of magma ascent in the Pinacate field resulted in bands of vents perhaps as much as a few kilometers wide, and it did not produce numerous extremely linear chains of vents. At least one of these bands represents a major fault zone. The northerly elongation of the field itself may reflect the geometry of its mantle magma source region.

Acknowledgments. We thank Chuck Connor and Tom Anderson for helpful discussions and Dazheng Zhang for assistance in the early stages of this research. The paper was significantly improved by the reviews of Chuck Connor, Leon Reiter, and William Melson.

References

Anderson, T.H., and L.T. Silver, An overview of Precambrian rocks in Sonora, *Rev. Univ. Nal. Auton. Mex. Inst. Geol., 5*, 131-139, 1981.

Connor, C.B., Cinder cone clustering in the TranMexican Volcanic Belt: Implications for structural and petrologic models, *J. Geophys. Res., 95*, 19,395-19,405, 1990.

Connor, C.B., C.D. Condit, L.S. Crumpler, and J.C. Aubele, Evidence of regional structural controls on vent distribution: Springerville volcanic field, Arizona, *J. Geophys. Res., 97*, 12,349-12,359, 1992.

Delaney, P.T., D.D. Pollard, J.I. Ziony, and E.H. McKee, Field relations between dikes and joints: Emplacement processes and paleostress analysis, *J. Geophys. Res., 91*, 4920-4938, 1986.

Donnelly, M.F., Geology of the Sierra del Pinacate volcanic field, northern Sonora, Mexico, and southern Arizona, U.S.A., Ph.D. thesis, 722 pp., Stanford Univ., Stanford, Calif., 1974.

Draper, G., Z. Chen, M. Conway, C.B. Connor, and C.D. Condit, Structural control of magma pathways in the upper crust: Insights from the San Francisco volcanic field, Arizona, *Geol. Soc. Am. Abstr. programs, 26*(7), A115, 1994.

Fehler, M., L. House, and H. Kaieda, Determining planes along which earthquakes occur: Method and application to earthquakes accompanying hydraulic fracturing, *J. Geophys. Res., 92*, 9407-9414, 1987.

Fenby, S.S., and R.G. Gastil, Geologic-tectonic map of the Gulf of California and Surrounding areas, *The Gulf and Peninsular Province of the Californias*, edited by J.P. Dauphin and B.R.T. Simoneit, *AAPG Mem. 47*, 79-83, 1991.

Gastil, R.G., and S.S. Fenby, Detachment faulting as a mechanism for tectonically filling the Gulf of California during dilation, *The Gulf and Peninsular Province of the Californias*, edited by J.P. Dauphin and B.R.T. Simoneit, *AAPG Mem. 47*, 371-375, 1991.

Gutmann, J.T., Geology of Crater Elegante, Sonora, Mexico, *Geol. Soc. Am. Bull., 87*, 1718-1729, 1976.

Gutmann, J.T., Structure and eruptive cycle of cinder cones in the Pinacate volcanic field and the controls of Strombolian activity, *J. Geol., 87*, 448-454, 1979.

Lutz, T.M., An analysis of the orientations of large-scale crustal structures: a statistical approach based on areal distributions of pointlike features, *J. Geophys. Res., 91*, 421-434, 1986.

Lynch, D.J., Genesis and geochronology of alkaline volcanism in the Pinacate volcanic field of northwestern Sonora, Mexico, Ph.D. thesis, 248 pp., Univ. of Ariz., Tucson, 1981.

Lynch, D.J., and J.T. Gutmann, Volcanic structures and alkaline rocks in the Pinacate volcanic field of Sonora, Mexico, *Spec. Pap. 5*, pp. 309-322, Ariz. Bur. of Geol. and Miner. Technol., Tucson, 1987.

McDuffie, S.M., C.B. Connor, and K.D. Mahrer, A simple 2-D stress model of dike-fracture interaction, *Eos Trans. AGU, 75*(16), Spring Meet. Suppl., 345, 1994.

Silverman, B.W., *Density Estimation for Statistics and Data Analysis*, 175 pp., Chapman and Hall, New York, 1986.

Slate, J.L., W.B. Bull, T.-L. Ku, M. Shafiqullah, D.J. Lynch, and Y.-P. Huang, Soil-carbonate genesis in the Pinacate volcanic field, northwestern Sonora, Mexico, *Quat. Res., 35*, 400-416, 1991.

Wadge, G., and A.M. Cross, Quantitative methods for detecting aligned points: An application to the volcanic vents of the Michoacan-Guanajuato volcanic field, Mexico, *Geology, 16*, 815-818, 1988.

Wadge, G., and A.M. Cross, Identification and analysis of the alignments of point-like features in remotely-sensed imagery: Volcanic cones in the Pinacate volcanic field, Mexico, *Int. J. Remote Sens., 10*, 455-474, 1989.

Zhang, D., Spatial patterns of magma emplacement and their relations to crustal structures: statistical and spectral methods and applications, Ph.D. thesis, 240 pp., Univ. of Pa., 1991.

Zhang, D., and T.M. Lutz, Structural control of igneous complexes and kimberlites: A new statistical method, *Tectonophysics, 159*, 137-148, 1989.

J.T. Gutmann, Department of Earth and Environmental Sciences, Wesleyan University, Middletown, CT 06459. (e-mail: jgutmann@eagle.wesleyan.edu)

T.M. Lutz, Department of Geology and Astronomy, West Chester University, West Chester, PA 19383. (e-mail: tlutz@wcupa.edu)

(Received May 18, 1994; received March 21, 1995;
accepted March 27, 1995.)